Exchange Biasing Single Molecule Magnets: Coupling of TbPc$_2$ to Antiferromagnetic Layers

A. Lodi Rizzini,[†] C. Krull,[†] T. Balashov,[†] A. Mugarza,[†] C. Nistor,[†] F. Yakhou,[‡] V. Sessi,[‡] S. Klyatskaya,[§] M. Ruben,[§,‖] S. Stepanow,[⊥] and P. Gambardella*,[†,#,∇]

[†]Catalan Institute of Nanotechnology (ICN), UAB Campus, E-08193 Barcelona, Spain

[‡]European Synchrotron Radiation Facility, BP 220, F-38043 Grenoble, France

[§]Institute of Nanotechnology, Karlsruhe Institute of Technology (KIT), D-76344 Eggenstein-Leopoldshafen, Germany

[‖]Institute de Physique et Chimie de Matériaux de Strasbourg (IPCMS), UMR 7504, CNRS-Université de Strasbourg, F-67034 Strasbourg, France

[⊥]Max-Planck-Institut für Festkörperforschung, D-70569 Stuttgart, Germany

[#]Institució Catalana de Recerca i Estudis Avançats (ICREA), E-08100 Barcelona, Spain

[∇]Departament de Física, Universitat Autònoma de Barcelona, E-08193 Barcelona, Spain

S *Supporting Information*

ABSTRACT: We investigate the possibility to induce exchange bias between single molecule magnets (SMM) and metallic or oxide antiferromagnetic substrates. Element-resolved X-ray magnetic circular dichroism measurements reveal, respectively, the presence and absence of unidirectional exchange anisotropy for TbPc$_2$ SMM deposited on anti-ferromagnetic Mn and CoO layers. TbPc$_2$ deposited on Mn thin films present magnetic hysteresis and a negative horizontal shift of the Tb magnetization loop after field cooling, consistent with the observation of pinned spins in the Mn layer coupled parallel to the Tb magnetic moment. Conversely, molecules deposited on CoO substrates present paramagnetic magnetization loops with no indication of exchange bias. These experiments demonstrate the ability of SMM to polarize the pinned uncompensated spins of an antiferromagnet during field-cooling and realize metal−organic exchange-biased heterostructures using antiferromagnetic pinning layers.

KEYWORDS: Single molecule magnets, TbPc$_2$, exchange bias, cobalt oxide, manganese, X-ray magnetic circular dichroism
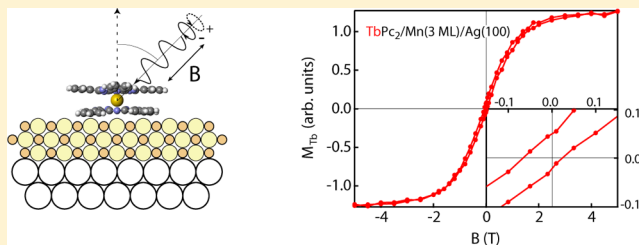
Exchange bias is a key phenomenon in spintronics that allows for the magnetization of thin ferromagnetic (FM) layers to be stabilized by exchange coupling to adjacent antiferromagnetic (AFM) layers.[1] Exchange bias typically occurs in either FM/AFM bilayers or FM/AFM core−shell nanoparticles cooled in a magnetic field from below the Curie temperature of the FM through the Néel temperature (T_N) of the AFM.[2,3] Unidirectional exchange anisotropy sets in below T_N, as the interfacial spins of the AFM align with the magnetization of the FM and henceforth remain pinned in the direction of the cooling field. The tell-tale signature of exchange bias is a shift of the hysteresis loop of the FM along the field axis by an amount H_E, termed the exchange field, often accompanied by an enhancement of the coercivity H_C. These effects offset the response of a FM to applied magnetic fields, currents, and temperature, leading to prominent applications of exchange bias in, for example, spin valve and magnetic tunnel junction devices.

While FM layers will remain the basic ingredient of storage and spintronic devices in the near future, size and power scaling trends call for radical changes in material design. Such changes could be achieved, in principle, by including molecular-scale elements in hybrid metal or semiconducting architectures.[4,5] Magnetic molecules are highly attractive in this sense, both as ordered two-dimensional films in multilayer structures[6] or as single magnetic units connected to microscopic electrodes.[7,8] For example, single molecule magnets (SMM) can be used to store one bit of information in an extremely small volume or act as efficient spin filters and injectors. However, to exploit the spin as a state variable, the molecular magnetic moment needs to survive the interaction with the substrate and be stabilized against thermal fluctuations. One of the critical issues in this field, therefore, is to achieve control over the electronic and magnetic coupling of molecular complexes to inorganic substrates.[9−13]

Recent experiments have shown that metal−organic molecules in physical contact with a FM may exhibit either ferromagnetic or antiferromagnetic coupling to a FM

substrate.[14−16] In the case of the TbPc$_2$ single molecule magnet (SMM),[17] it has been shown that the competition between substrate-induced exchange coupling, Zeeman interaction, and magnetic anisotropy gives rise to several metastable magnetic configurations of the SMM/FM interface.[10] However, the possibility of inducing exchange bias between a molecule and an AFM has not been reported thus far. There are actually specific reasons that put *molecular exchange bias* into question. First, exchange bias is triggered locally by the presence of pinned uncompensated spins in the AFM.[18−20] As the molecules constitute discrete magnetic elements, there is no mechanism guaranteeing that the sparse pinning centers of an AFM may bias a single molecule, unless this adsorbs on or creates a pinning site. Second, biasing is unlikely to extend from individual sites to a continuous molecular layer, since the magnetic moments of molecules adsorbed next to each other are usually uncoupled.[21] Third, thermal fluctuations tend to randomize the orientation of the molecular magnetic moment down to temperatures $T \ll T_N$, which hinders the alignment of the pinned spins in the AFM during the field cooling (FC) process.

In this work we present a series of experiments aimed at establishing the presence or absence of molecular exchange bias at the interface between TbPc$_2$ and different types of AFM substrates, namely, insulating CoO and metallic Mn thin films deposited on a single crystal Ag(100) surface. Despite the unfavorable premises discussed above, we find that exchange bias can be induced in TbPc$_2$ adsorbed on Mn, resulting in enhanced coercivity and a shifted hysteresis loop of the molecular magnetization. Only a fraction of the TbPc$_2$ molecules appear to be biased, however, which calls for further investigations of the microscopic mechanism leading to the pinning of molecular spins. These results will help to address several outstanding problems in the field of molecular spintronics related to the incorporation of magnetic molecules in practical devices. The pinning of SMM, and paramagnetic molecules in general, to AFM represents a convenient way to stabilize and control their magnetic properties using substrates with no net magnetization.

The choice of AFM substrate is a critical issue in our search for molecular exchange bias, given that the superexchange interaction between molecule and surface spins depends on the chemistry of the interfacial bonds.[10,15] We selected CoO and Mn as representative materials for AFM oxides and metals, respectively. CoO is a model type II insulating AFM that grows epitaxially on Ag(100). Its choice was motivated by its large magnetocrystalline anisotropy, which is known to favor large H_E and H_C in FM/AFM bilayers. Moreover, both T_N and the magnetic anisotropy of CoO thin films can be controlled by epitaxy,[22,23] which makes this system particularly interesting for the investigation of molecular exchange bias phenomena. Elemental Mn thin films grown on Ag(100)[24−26] were preferred over other types of metallic AFM, such as NiMn and IrMn, to simplify the sample preparation procedure, minimize chemical disorder at the SMM/AFM interface, and avoid the presence of different structural and magnetic phases that appear in bimetallic AFM alloys as a function of composition and thickness.[27] Mn layers grow epitaxially on single crystal Ag(100) forming a two-layer thick superficial alloy at room temperature, which is continued by an almost pure Mn phase with bct structure above the third layer.[26,28] It is known that Mn thin films grown on Ag(100) present large local magnetic moments and AFM order,[25,29,30] with a predicted $c(2$

× 2) magnetic unit cell.[30,31] The spin alignment in the top surface layer of our films, however, could not be determined experimentally and remains unknown (see Supporting Information). The TbPc$_2$/CoO/Ag and TbPc$_2$/Mn/Ag samples were grown in situ by molecular beam epitaxy in ultrahigh-vacuum (UHV) by evaporating Co in a pure oxygen atmosphere of 10^{-7} mbar[32] or Mn on a clean Ag(100) substrate at room temperature.[26,28] About 0.5 monolayers (1 ML = 1.5×10^{14} molecules cm^{-2}) of TbPc$_2$ molecules were deposited on each substrate, by sublimation of the molecular powder in UHV. The thickness of the AFM and the coverage of TbPc$_2$ were monitored in situ using scanning tunnelling microscopy (Supporting Information). Polarization-dependent X-ray absorption measurements were performed at beamline ID08 of the European Synchrotron Radiation Facility using total electron yield detection at the $L_{2,3}$ edges of Co and Mn and the $M_{4,5}$ edges of Tb. X-ray absorption spectra (XAS) with linearly polarized light were used in addition to STM to characterize the growth and AFM properties of the CoO layers (Supporting Information). A magnetic field **B** of up to ±5 T was applied parallel to the X-ray incidence direction at an angle θ with respect to the sample normal and used for FC the samples as well as for X-ray magnetic circular dichroism (XMCD) measurements. XMCD spectra were obtained by subtracting consecutive absorption spectra recorded for parallel (I^+) and antiparallel (I^-) alignment of the photon helicity and sample magnetization. We recall that the XMCD intensity can be directly related to the expectation value of the magnetic moment of the element under investigation by using a set of sum rules.[33,34] Element resolved magnetization curves were measured by averaging up to 16 XMCD spectra per point and reporting the XMCD intensity at the M_5 (L_3) edge of Tb (Mn) as a function of applied magnetic field. Throughout this work, the XMCD signal is presented in units of the average XAS intensity, $(I^+ + I^-)/2$. For more details about the TbPc$_2$ deposition, beamline setup, and XMCD measurements we refer to the Supporting Information and refs 35 and 36.
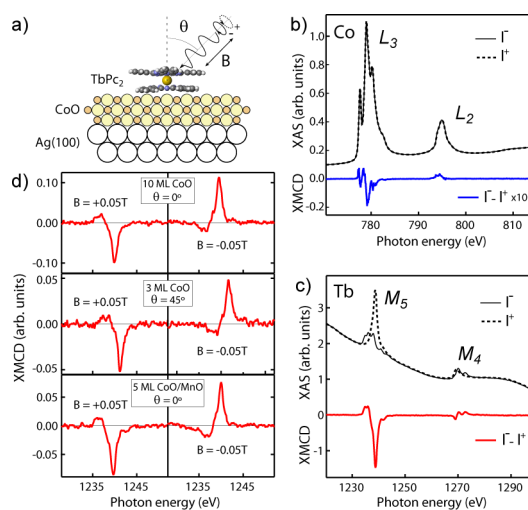

Figure 1. (a) Schematic of TbPc$_2$ deposited on CoO/Ag(100). (b,c) XAS and XMCD spectra of TbPc$_2$/CoO(10 ML)/Ag recorded at the $L_{2,3}$ Co (b) and $M_{4,5}$ Tb (c) edges after FC at $B = 5$ T, $\theta = 0°$, and $T = 8$ K. (d) XMCD intensity of the M_5 Tb edge measured at $B = \pm 0.05$ T, $T = 8$ K on TbPc$_2$/CoO (10 ML) (top), TbPc$_2$/CoO (3 ML) (middle), and TbPc$_2$/CoO (5 ML)/MnO (45 ML) (bottom).

We present first the results obtained for TbPc$_2$ deposited on a 10 ML thick CoO layer (Figure 1a). The CoO substrate presents a very weak field-induced XMCD (Figure 1b), measured at the $L_{2,3}$ edges of Co after FC from 300 to 8 K at B = +5 T and θ = 0°, as expected for a nominally compensated AFM surface. The nonzero XMCD intensity is attributed to the presence of rotatable uncompensated Co spins polarized by the external field. The TbPc$_2$ molecules, on the other hand, present a very large XMCD signal (Figure 1c), which is fully saturated at 5 T. To verify the presence of exchange bias, we measured the intensity of the Tb XMCD during a +B→−B field sweep on either side of B = 0. Figure 1d shows that the XMCD spectra recorded at B = +0.05 and −0.05 T reverse sign and have a similar intensity, indicating that the Tb magnetization is antisymmetric with respect to the origin. This finding is confirmed by the measurement of a complete magnetization cycle (Figure 2a), which yields a reversible and
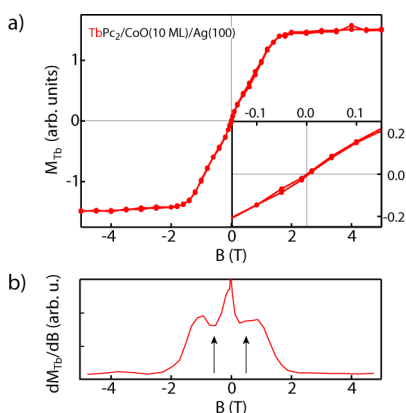

Figure 2. (a) Magnetization loop of TbPc$_2$ deposited on a 10 ML CoO film after FC at θ = 0° and B = 5 T, recorded at θ = 0° and T = 8 K. Inset: Detail of the low field region. Units refer to the intensity ratio $2(I^+ - I^-)/(I^+ + I^-)$ measured at the M_5 Tb edge. (b) Derivative of the magnetization shown in part a. The arrows indicate the position of local minima.

antisymmetric loop and no indication of exchange bias (inset). Such paramagnetic behavior is consistent with that of TbPc$_2$ molecules deposited on nonmagnetic substrates, which do not show hysteresis at T = 8 K.[35,37] Note that the Tb loop presents inflection points at B = ± 0.5 T, indicated by minima in the derivative of the magnetization (arrows in Figure 2b), which are reminiscent of the plateaus of the "butterfly" hysteresis cycle of TbPc$_2$ measured below the blocking temperature in molecular crystals.[38] These features, which are absent for TbPc$_2$ deposited on metallic surfaces,[10,35,37] suggest that the electronic interaction between molecules and substrate is rather weak.

Several reasons may explain the absence of exchange bias for TbPc$_2$ on CoO. The first is that the magnetic moment of TbPc$_2$ fluctuates during FC, so that the effective exchange field at the SMM/AFM interface averages out as the temperature drops below T_N. Although we did not measure T_N during this experiment, this hypothesis was tested by decreasing the thickness of CoO down to 3 ML, which is expected to reduce T_N to about 20 K due to finite-size effects.[22] The middle panels of Figure 1d show the XMCD spectra of TbPc$_2$/CoO(3 ML)/Ag recorded at B = ±0.05 T after FC at B = +5 T and θ = 45°. We used this geometry to probe simultaneously the out-of-plane and in-plane magnetization since, a priori, it is not known which direction may be favored. We find that the XMCD is still

antisymmetric with respect to B, giving no indication of exchange bias. A second possibility is that the easy axes of TbPc$_2$ and CoO are perpendicular to each other and the magnetic anisotropy stronger than Tb−Co exchange, in which case the bias field will essentially have no effect. Indeed, while the spins of bulk CoO align close to the (111) direction,[39] compressive strain is expected to favor preferential in-plane orientation of the magnetic moments in CoO/Ag(100),[23] perpendicular to the TbPc$_2$ easy axis. It is possible, however, to induce out-of-plane alignment of the Co spins by growing tensile-strained CoO on MnO/Ag(100).[23] We have thus grown a 5 ML thick film of CoO on 45 ML MnO/Ag(100) with out-of-plane magnetic anisotropy (Supporting Information). Also in this case, however, the XMCD spectra measured after FC at B = ± 0.05 T and θ = 0° present a similar intensity and opposite sign (Figure 1d, bottom panels), revealing no hint of exchange bias. We must conclude, therefore, that the exchange coupling between TbPc$_2$ and CoO is too weak to produce sizable bias effects, at least within the sensitivity of the present study.

Since the exchange interaction between TbPc$_2$ and a FM was previously found to be larger for pure metal substrates compared to oxidized surfaces,[10] we turned our investigation toward metallic AFM. We thus deposited TbPc$_2$ on a 3 ML-thick Mn film grown on Ag(100) and FC it to 8 K at B = +5 T and θ = 0°. Figure 3a shows that the field-induced XMCD
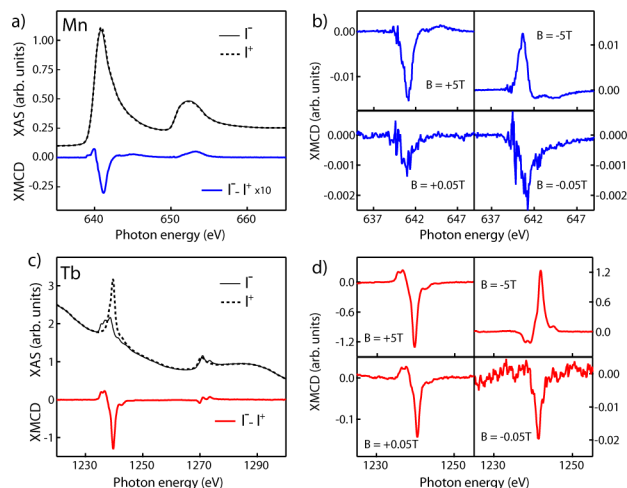

Figure 3. XAS and XMCD spectra of TbPc$_2$/Mn(3 ML)/Ag recorded after FC at B = 5 T, θ = 0°, and T = 8 K. (a) $L_{2,3}$ edges. (b) XMCD intensity at the L_3 Mn edge as a function of applied field. (c) $M_{4,5}$ Tb edges. (d) XMCD intensity at the M_5 Tb edge as a function of applied field.

measured at 5 T at the $L_{2,3}$ Mn edges is extremely small compared to that of paramagnetic Mn samples measured in similar conditions, for which an XMCD asymmetry of the order of 50% of the total XAS is expected.[40] Likewise, the presence of Mn clusters[41] or of a spurious ferromagnetic phase[42] is extremely unlikely. This indicates that the Mn layer is AFM, as expected. By reducing B from +5 to +0.05 T, we observe a 10-fold reduction of the XMCD intensity. Most importantly, when reversing the field to B = −0.05 T, the sign of the XMCD remains negative, whereas the XMCD measured at −5 T reverses sign but is smaller by 14% with respect to that measured at +5 T (Figure 3b). This behavior suggests the presence of uncompensated Mn spins, part of which rotate with the field and part pinned parallel to the FC direction. The

vertical shift of the Mn magnetization loop, shown in Figure 4a, confirms the presence of pinned Mn spins. The ratio between
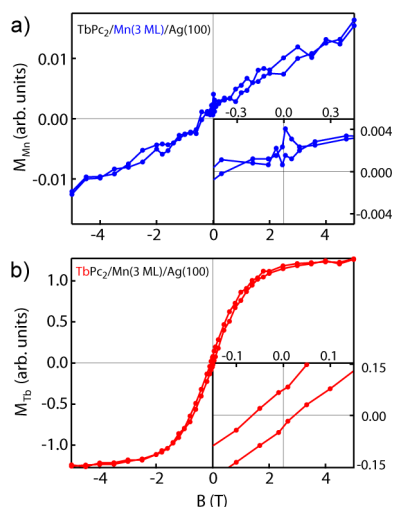

Figure 4. Magnetization loops of Mn (a) and Tb (b) measured on $TbPc_2/Mn(3 ML)/Ag(100)$, after FC at $\theta = 0°$ and $B = 5$ T, recorded at $\theta = 0°$ and $T = 8$ K. Inset: Detail of the low field region. Units refer to the intensity ratio $2(I^+ - I^-)/(I^+ + I^-)$ measured at the L_3 Mn edge (a) and M_5 Tb edge (b).

loop shift and height indicates that about $(7 \pm 2)\%$ of the total uncompensated moments are pinned. By comparing the average spin magnetic moment of Mn, derived by applying the XMCD spin sum rule[34] to the spectra of Figure 3a, with that calculated for Mn in AFM layers,[25,30] we estimate that the percentage of uncompensated spins (pinned and unpinned) is about $(3 \pm 1)\%$ of the total Mn coverage, that is, 0.09 ± 0.03 ML (Supporting Information).

The remaining point is whether the $TbPc_2$ molecules couple to the pinned Mn spins, leading to exchange bias. Figure 3c shows the XAS and XMCD spectra of Tb measured after FC, which are very similar to those reported for CoO (Figure 1c). Yet, we find that the Tb XMCD does not reverse sign going from $B = +0.05$ to -0.05 T (Figure 3d), opposite to the behavior observed on CoO and similar to the Mn spectra (Figure 3b). The measurement of the Tb magnetization loop provides final evidence of exchange bias in this system. Figure 4b reveals that, while $TbPc_2$ on CoO presents a closed loop, the magnetization of $TbPc_2$ on Mn is hysteretic and exhibits finite remanence and coercivity $H_C = 44 \pm 4$ mT. Furthermore, the Tb magnetization is negatively shifted along the field axis by an amount $H_E = -22 \pm 4$ mT. The sign of the shift is consistent with the parallel alignment of the Tb magnetic moment and pinned Mn spins evidenced by the low field XMCD spectra reported in Figure 3b and d.

From the skewed shape of the loop and the small remanence value, it is evident that only a small fraction of the $TbPc_2$ molecules is exchange-coupled to the substrate, consistent with the presence of a small percentage of pinned spins. This is very different from the case of $TbPc_2$ deposited on Ni, where all of the molecules are coupled to the FM, and a squared hysteresis loop with 100% remanence is observed.[10] As XMCD averages over a macroscopic sample area, it is likely that both H_E and H_C would be much larger if measured at the single molecule level. We note also that the blocking temperature of $TbPc_2$ deposited on metal substrates, measured on the time scale of XMCD

experiments, is about 2 K,[37] below the minimum temperature reached in this study (8 K). Therefore, the alignment of the pinned spins must occur in the paramagnetic regime[43] due to the field-induced magnetization of $TbPc_2$. Once AFM order has set in, the uncompensated exchange field from the substrate inhibits the relaxation of the Tb magnetic moment, giving rise to hysteresis. Remarkably, both H_C and H_E decrease significantly for a $TbPc_2/Mn$ sample FC at $\theta = 90°$, perpendicular to the $TbPc_2$ easy axis (Supporting Information). We attribute this behavior to the smaller polarization of the molecular magnetic moment induced by the external field in this geometry, which hinders the pinning of neighbor uncompensated Mn spins parallel to the FC direction.

In summary, we have reported exchange bias in a SMM/AFM system. The magnetization of $TbPc_2$ deposited on CoO and Mn thin films, FC to 8 K, present significant differences: the first is typical of paramagnetic $TbPc_2$, whereas the second is an hysteretic loop shifted to negative field. The Mn magnetization loop reveals the presence of both pinned and unpinned spins, with the former aligned parallel to the FC direction. Thus, molecular scale magnets are able to polarize the pinned spins of an AFM during FC, which induce exchange bias of the molecules to the substrate. The bias field is found to be maximum when the cooling field is set parallel to the SMM easy axis. From the shape of the $TbPc_2$ magnetization curve, we infer that exchange bias occurs at the level of single molecules. Control over the origin of the pinned spins and positioning of the molecules may result in new applications that exploit the interaction between SMM and AFM, such as spin valves and spin filters, where the molecular magnetic moment is simultaneously stabilized and biased by unidirectional exchange coupling.

■ ASSOCIATED CONTENT

Ⓢ Supporting Information
Sample characterization, details of XMCD measurements, and analysis of the uncompensated Mn moments. This material is available free of charge via the Internet at http://pubs.acs.org.

■ AUTHOR INFORMATION

Corresponding Author
*E-mail: pietro.gambardella.icn@uab.es.
Notes
The authors declare no competing financial interest.

■ ACKNOWLEDGMENTS

■ REFERENCES

(1) Parkin, S.; Jiang, X.; Kaiser, C.; Panchula, A.; Roche, K.; Samant, M. *Proc. IEEE* **2003**, *91*, 661−680.
(2) Meiklejohn, W. H.; Bean, C. P. *Phys. Rev.* **1957**, *105*, 904−913.
(3) Nogués, J.; Sort, J.; Langlais, V.; Skumryev, V.; Suriñach, S.; Muñoz, J.; Baró, M. *Phys. Rep.* **2005**, *422*, 65−117.
(4) Stan, M.; Franzon, P.; Goldstein, S.; Lach, J.; Ziegler, M. *Proc. IEEE* **2003**, *91*, 1940−1957.
(5) Joachim, C.; Ratner, M. A. *Proc. Natl. Acad. Sci. U.S.A.* **2005**, *102*, 8801−8808.

(6) Dediu, V. A.; Hueso, L. E.; Bergenti, I.; Taliani, C. *Nat. Mater.* **2009**, *8*, 850−850.

(7) Bogani, L.; Wernsdorfer, W. *Nat. Mater.* **2008**, *7*, 179−186.

(8) Urdampilleta, M.; Klyatskaya, S.; Cleuziou, J.-P.; Ruben, M.; Wernsdorfer, W. *Nat. Mater.* **2011**, *10*, 502−506.

(9) Moth-Poulsen, K.; Bjornholm, T. *Nat. Nanotechnol.* **2009**, *4*, 551−556.

(10) Lodi Rizzini, A.; Krull, C.; Balashov, T.; Kavich, J. J.; Mugarza, A.; Miedema, P. S.; Thakur, P. K.; Sessi, V.; Klyatskaya, S.; Ruben, M.; Stepanow, S.; Gambardella, P. *Phys. Rev. Lett.* **2011**, *107*, 177205.

(11) Mugarza, A.; Krull, C.; Robles, R.; Stepanow, S.; Ceballos, G.; Gambardella, P. *Nat. Commun.* **2011**, *2*, 490.

(12) Miyamachi, T.; Gruber, M.; Davesne, V.; Bowen, M.; Boukari, S.; Joly, L.; Scheurer, F.; Rogez, G.; Yamada, T. K.; Ohresser, P.; Beaurepaire, E.; Wulfhekel, W. *Nat. Commun.* **2012**, *3*, 938.

(13) Schwöbel, J.; Fu, Y.; Brede, J.; Dilullo, A.; Hoffmann, G.; Klyatskaya, S.; Ruben, M.; Wiesendanger, R. *Nat. Commun.* **2012**, *3*, 953.

(14) Scheybal, A.; Ramsvik, T.; Bertschinger, R.; Putero, M.; Nolting, F.; Jung, T. *Chem. Phys. Lett.* **2005**, *411*, 214−220.

(15) Bernien, M.; Miguel, J.; Weis, C.; Ali, M. E.; Kurde, J.; Krumme, B.; Panchmatia, P. M.; Sanyal, B.; Piantek, M.; Srivastava, P.; Baberschke, K.; Oppeneer, P. M.; Eriksson, O.; Kuch, W.; Wende, H. *Phys. Rev. Lett.* **2009**, *102*, 047202.

(16) Javaid, S.; Bowen, M.; Boukari, S.; Joly, L.; Beaufrand, J.-B.; Chen, X.; Dappe, Y. J.; Scheurer, F.; Kappler, J.-P.; Arabski, J.; Wulfhekel, W.; Alouani, M.; Beaurepaire, E. *Phys. Rev. Lett.* **2010**, *105*, 077201.

(17) Ishikawa, N.; Sugita, M.; Ishikawa, T.; Koshihara, S.; Kaizu, Y. *J. Am. Chem. Soc.* **2003**, *125*, 8694−8695.

(18) Takano, K.; Kodama, R. H.; Berkowitz, A. E.; Cao, W.; Thomas, G. *Phys. Rev. Lett.* **1997**, *79*, 1130−1133.

(19) Ohldag, H.; Scholl, A.; Nolting, F.; Arenholz, E.; Maat, S.; Young, A. T.; Carey, M.; Stöhr, J. *Phys. Rev. Lett.* **2003**, *91*, 017203.

(20) Noguès, J.; Stepanow, S.; Bollero, A.; Sort, J.; Dieny, B.; Nolting, F.; Gambardella, P. *Appl. Phys. Lett.* **2009**, *95*, 152515.

(21) Gambardella, P.; et al. *Nat. Mater.* **2009**, *8*, 189−193.

(22) Ambrose, T.; Chien, C. L. *Phys. Rev. Lett.* **1996**, *76*, 1743−1746.

(23) Csiszar, S. I.; Haverkort, M. W.; Hu, Z.; Tanaka, A.; Hsieh, H. H.; Lin, H.-J.; Chen, C. T.; Hibma, T.; Tjeng, L. H. *Phys. Rev. Lett.* **2005**, *95*, 187205.

(24) Jonker, B. T.; Krebs, J. J.; Prinz, G. A. *Phys. Rev. B* **1989**, *39*, 1399−1402.

(25) Blügel, S.; Dederichs, P. H. *Europhys. Lett.* **1989**, *9*, 597−602.

(26) Schieffer, P.; Tuilier, M.-H.; Hanf, M.-C.; Krembel, C.; Gewinner, G. *Surf. Sci.* **1999**, *422*, 132−140.

(27) Massalski, T.; Murray, J.; Bennett, L.; Baker, H. *Binary alloy phase diagrams*; Binary Alloy Phase Diagrams v. 2; American Society for Metals: Russell Township, OH, 1986.

(28) Schieffer, P.; Hanf, M.; Krembel, C.; Gewinner, G. *Surf. Sci.* **2000**, *446*, 175−186.

(29) Schieffer, P.; Krembel, C.; Hanf, M.-C.; Tuilier, M.-H.; Wetzel, P.; Gewinner, G.; Hricovini, K. *Eur. Phys. J. B* **1999**, *8*, 165−168.

(30) Krüger, P.; Elmouhssine, O.; Demangeat, C.; Parlebas, J. C. *Phys. Rev. B* **1996**, *54*, 6393−6400.

(31) Hafner, J.; Spišák, D. *Phys. Rev. B* **2005**, *72*, 144420.

(32) Sebastian, I.; Bertrams, T.; Meinel, K.; Neddermeyer, H. *Faraday Discuss.* **1999**, *114*, 129−140.

(33) Thole, B. T.; Carra, P.; Sette, F.; van der Laan, G. *Phys. Rev. Lett.* **1992**, *68*, 1943−1946.

(34) Carra, P.; Thole, B. T.; Altarelli, M.; Wang, X. *Phys. Rev. Lett.* **1993**, *70*, 694−697.

(35) Stepanow, S.; Honolka, J.; Gambardella, P.; Vitali, L.; Abdurakhmanova, N.; Tseng, T.-C.; Rauschenbach, S.; Tait, S. L.; Sessi, V.; Klyatskaya, S.; Ruben, M.; Kern, K. *J. Am. Chem. Soc.* **2010**, *132*, 11900−11901.

(36) Stepanow, S.; Mugarza, A.; Ceballos, G.; Moras, P.; Cezar, J. C.; Carbone, C.; Gambardella, P. *Phys. Rev. B* **2010**, *82*, 014405.

(37) Margheriti, L.; Chiappe, D.; Mannini, M.; Car, P.-E.; Sainctavit, P.; Arrio, M.-A.; de Mongeot, F. B.; Cezar, J. C.; Piras, F. M.; Magnani, A.; Otero, E.; Caneschi, A.; Sessoli, R. *Adv. Mater.* **2010**, *22*, 5488−5493.

(38) Ishikawa, N.; Sugita, M.; Wernsdorfer, W. *Angew. Chem.* **2005**, *44*, 2931−2935.

(39) Jauch, W.; Reehuis, M.; Bleif, H. J.; Kubanek, F.; Pattison, P. *Phys. Rev. B* **2001**, *64*, 052102.

(40) Gambardella, P.; Brune, H.; Dhesi, S. S.; Bencok, P.; Krishnakumar, S. R.; Gardonio, S.; Veronese, M.; Grazioli, C.; Carbone, C. *Phys. Rev. B* **2005**, *72*, 045337.

(41) Rader, O.; Gudat, W.; Schmitz, D.; Carbone, C.; Eberhardt, W. *Phys. Rev. B* **1997**, *56*, 5053−5056.

(42) O'Brien, W. L.; Tonner, B. P. *Phys. Rev. B* **1995**, *51*, 617−620.

(43) Cai, J. W.; Liu, K.; Chien, C. L. *Phys. Rev. B* **1999**, *60*, 72−75.